Published in final edited form as:
J Cell Physiol. 2011 April ; 226(4): 1082–1089. doi:10.1002/jcp.22423.

The Role of Calcium Release Activated Calcium Channels in Osteoclast Differentiation

Yandong Zhou[#3], **Tricia L. Lewis**[#1], **Lisa J. Robinson**[2], **Kathy M. Brundage**[1,4], **Rosana Schafer**[1], **Karen H. Martin**[1,4], **Harry C Blair**[2], **Jonathan Soboloff**[3], and **John B. Barnett**[1,4]

[1]Department of Microbiology, Immunology & Cell Biology, West Virginia University School of Medicine, Morgantown, WV 26506.

[2]Departments of Pathology and Physiology & Cell Biology, University of Pittsburgh School of Medicine, and Veteran's Affairs Medical Center, Pittsburgh, PA 15216.

[3]Department of Biochemistry, Temple University School of Medicine, Philadelphia, PA 19140.

[4]Mary Babb Randolph Cancer Center, West Virginia University School of Medicine, Morgantown, WV 26506.

[#] These authors contributed equally to this work.

Abstract

Osteoclasts are specialized macrophage derivatives that secrete acid and proteinases to mobilize bone for mineral homeostasis, growth, and replacement or repair. Osteoclast differentiation generally requires the monocyte growth factor m-CSF and the TNF-family cytokine RANKL, although differentiation is regulated by many other cytokines and by intracellular signals, including Ca^{2+}. Studies of osteoclast differentiation in vitro were performed using human monocytic precursors stimulated with m-CSF and RANKL, revealing significant loss in both the expression and function of the required components of store-operated Ca^{2+} entry over the course of osteoclast differentiation. However, inhibition of CRAC using either the pharmacological agent 3,4 dichloropropioanilide (DCPA) or by knockdown of Orai1 severely inhibited formation of multinucleated osteoclasts. In contrast, no effect of CRAC channel inhibition was observed on expression of the osteoclast protein tartrate resistant acid phosphatase (TRAP). Our findings suggest that despite the fact that they are downregulated during osteoclast differentiation, CRAC channels are required for cell fusion, a late event in osteoclast differentiation. Since osteoclasts cannot function properly without multinucleation, selective CRAC inhibitors may have utility in management of hyperresorptive states.

Keywords

Osteopetrosis; osteoporosis; Orai1; STIM1; cell fusion; 3,4 dichloropropioanilide

Correspondence: John B. Barnett, Ph.D. Dept of Microbiol, Immunol and Cell Biol WVU School of Medicine One Medical Center Drive Morgantown, WV 26506. (T) 304-293-4029 (F) 304-293-7823 jbarnett@hsc.wvu.edu or Jonathan Soboloff, Ph.D. Department of Biochemistry Temple University School of Medicine 3440 N. Broad Street Philadelphia, PA 19140 (T) 215-707-6567 (F) 215-707-7536 soboloff@temple.edu.

Introduction

Osteoclast differentiation from monocytes and regulation of attachment to bone are dependent on inositol-1,3,5 trisphosphate ($InsP_3$)-mediated Ca^{2+}-release from the endoplasmic reticulum (ER) (Blair et al, 2007; Koga et al, 2004; Kim et al, 2005). Less clear is the extent to which extracellular Ca^{2+} influx is involved osteoclast differentiation. In hematopoietic cells, Ca^{2+}-Release-Activated Ca^{2+} (CRAC) channel activity represents the major means of Ca^{2+} entry (Deng et al, 2009; Feske, 2009). Further, the type 1A transmembrane protein STIM1 (Liou et al, 2005; Roos et al, 2005) and the plasma membrane Ca^{2+} channel Orai1 (Feske et al, 2006; Vig et al, 2006) have been defined as the molecular mediators of CRAC channel activity.

In CRAC channel activation, the ER luminal portion of the activating protein STIM1, which contains a low-affinity Ca^{2+}-binding EF hand (Stathopulos et al, 2006), mediates activation of Orai1 at the cell membrane. In this process, ER Ca^{2+} release, via $InsP_3$ receptors typically, causes a STIM1 conformational change (Stathopulos et al, 2008) that causes STIM1 aggregation at sites adjacent to the plasma membrane commonly referred to as puncta (Liou et al, 2005; Wu et al, 2006). At puncta the cytoplasmic membrane portion of STIM1 physically interacts with the plasma membrane-localized Ca^{2+} channel Orai1 resulting in its activation (Muik et al, 2009; Park et al, 2009; Wang et al, 2009; Yuan et al, 2009). The extent to which this pathway is active during osteoclast differentiation is not established.

We studied Orai1 and STIM1 expression and function during osteoclast differentiation in vitro, and found significant decreases early in the process of osteoclast differentiation. Further, reduction of Orai1 expression with siRNA inhibited osteoclast differentiation, particularly multinucleation. Intriguingly, the addition of the pharmacological agent 3,4-dichloropropioanilide (DCPA) similarly inhibited terminal osteoclast differentiation. We further establish that DCPA-mediated CRAC channel inhibition occurs via inhibition of STIM1-Orai1 interaction. DCPA is a haloanilide compound with relatively low systemic toxicity that can inhibit Ca^{2+} influx in macrophages and T cells as well as having potent anti-inflammatory activity (Xie et al, 1997; Ustyugova et al, 2007; Lewis et al, 2008). As such, our findings may have significant therapeutic implications.

Materials and Methods

Cell culture, cell lines, and cell differentiation in vitro

Human monocytes were isolated from normal buffy coat cells (60-80 ml) obtained with approval of institutional review boards by separation from donor blood, the white-cell depleted blood retained for clinical use. Human monocyte culture and differentiation were as reported (Yaroslavskiy et al, 2005). Briefly, human monocytes cells were isolated from buffy coat on ficoll lymphocyte separation media and cultured at ~6×10^5 cells per cm^2 in monocyte maintenance medium, Dulbecco's modified essential medium (DMEM) with 20 ng/ml of human m-CSF and 10% FBS), for 24 hours. After 24 hours in culture, the medium was changed to osteoclast differentiation medium containing in addition of human 50 ng/ml of RANKL, with the additional inhibitors or activators as specified in results. Human

osteoclast cultures were generally maintained for a minimum of seven days before analysis, or longer times as specified in results. Characterization of osteoclasts included in situ demonstration of tartrate resistant acid phosphatase (TRAP) using naphthol phosphate substrate coupled with fast garnet at pH 5 in 200 mM tartrate (Leucocyte acid phosphatase, Sigma-Aldrich, St. Louis, MO) and by evaluation of multinucleation using either phase contrast microscopy or nuclear stains.

Western Blots

Cells were lysed in 1% NP-40 (nonyl phenoxylpolyethoxylethanol), 150 mM NaCl, 50 mM Tris, pH 8.0, with proteinase inhibitors, cleared by centrifugation, and normalized for protein, determined by Bradford dye-binding. Proteins were resolved by electrophoresis on 8% polyacrylamide in sulfonlyl dodecyl sulfate, and transferred to polyvinylidene difluoride derivitized nylon. Membranes were blocked in Tris-buffered saline with 0.05% polyoxyethylene sorbitan (Tween 20) with 5% bovine serum albumin, 1 hour, 20°C, and incubated with the primary antibodies at 4 °C overnight. Membranes were washed and the appropriate peroxidase-conjugated secondary antibody added. After a 30 minute incubation, membranes were washed and bands were visualized by enhanced chemiluminescence (ECL-Western Blot Reagent Kit, GE Healthcare, Waukesha, WI).

Electrophysiology

Analysis was performed in HEK293 cells stably expressing Orai1 and transfected with STIM1 YFP used conventional whole cell voltage recordings as described (Wang et al, 2009). Immediately after establishment of the whole-cell electrode seal, voltage ramps spanning from -100 to +100 mV in 50 ms were delivered from a holding potential of 0 mV at a rate of 0.5 Hz. A 10 mV junction potential compensation were applied. The intracellular solution contained 145 mM CsGlu, 10 mM HEPES, 10 mM EGTA, 8 mM NaCl, 6 mM MgCl2, and 2 mM Mg-ATP (total 8 mM Mg^{2+}), pH 7.2; TRPM7 activity was suppressed by 8 mM Mg^{2+} and ATP (Zhou et al, 2009). The extracellular solution contained 145 mM NaCl, 10 mM CaCl2, 10 mM CsCl, 2 mM MgCl2, 2.8 mM KCl, 10 mM HEPES, and 10 mM glucose, pH 7.4.

DNA and RNA reagents

PCR primers: Homo sapiens Ca^{2+} release-activated Ca^{2+} modulator 1 (ORAI1) NM_032790: f: 5′- TCTCAACTCGGTCAAGGAGTC r: 5′- TTGAGGGGCAAGAACTTGACC; product 141 bp. Homo sapiens glyceraldehyde-3-phosphate dehydrogenase (GAPDH) NM_002046: f: 5′- ACAGTCAGCCGCATCTTCTT r: 5′- GACAAGCTTCCCGTTCTCAG; product 259 bp. Orai1 silencing used a pool of four siRNAs targeting homo sapiens ORAI1 (GenBank NM_032790), purchased as a pretested reagent from Dharmacon RNAi Technologies (smartpool 84876, Thermo-Fisher, Waltham MA). Cells were transfected using siPORTAmine (Ambion), a blend of polyamines, as described (Yaroslavskiy et al, 2005). Controls were transfected with nonsense siRNA. The siRNAs for Orai 5′ untranslated or open reading frame were GCUCACUGGUUAGCCAUAA, GGCCUGAUCUUUAUCGUCU GCACCUGUUUGCGCUCAUG, CAGCAUUGAGUGUGUACAU To visualize transfection, Cy5 was covalently attached to the duplex siRNA (Ambion Silencer siRNA

labeling kit, Austin, TX). mRNA was quantified by real-time PCR as described in Robinson et al. (2009).

STIM1 puncta formation

HEK293 cells, maintained in DMEM with 10% FBS, were transfected with YFP-STIM1 using Lipofectamine 2000 (Invitrogen, Carlsbad, CA) for 5 hours (37°C; 5% CO_2) followed by a 24 hour recovery. Cells were placed in 140 mM NaCl, 5 mM KCl, 1 mM $MgCl_2$, 10 mM glucose, 15 mM Hepes, 0.1 % BSA, 2 mM $CaCl_2$ and analyzed by confocal microscopy for STIM1 puncta formation using a Nikon phase-fluorescence microscope with CCD detectors (Diagnostic Instruments, Sterling Heights, MI). Phase or transmitted light microscopy used 10x-40x objectives and red, green, and blue filters to assemble color images. Fluorescence images used 1.4 NA 40x oil objectives. Red fluorescence used excitation at 530-560 nm, a 575 nm dichroic mirror, and 580-650 nm emission filter. Transfection data were analyzed using Nikon NIS Elements Imaging Software. The effect of DCPA on STIM1/Orai1 association was determined in wild-type HEK293 cells transfected with STIM1-YFP as described (Wang et al, 2009). Experiments were performed on a Leica DMI 6000B fluorescence microscope controlled by Slidebook Software (Intelligent Imaging Innovations; Denver, CO).

Cytosolic Ca^{2+} Measurement

Ratiometric imaging of intracellular Ca^{2+} using fura-2 was as described (Zhou et al, 2009). Briefly, cells on coverslips, in cation safe solution (107 mM NaCl, 7.2 mM KCl, 1.2 mM $MgCl_2$, 11.5 mM glucose, 20 mM Hepes-NaOH, pH 7.2) were loaded with fura-2 acetoxymethyl ester (2 μM) for 30 minutes at 24°C. Cells were washed and fluorescent probe was allowed to de-esterify for 30 minutes. From signal remaining after saponin permeabilization, ~85% of the dye was confined to the cytoplasm (Ma et al, 2000). Ca^{2+} measurements were made using a Leica DMI 6000B fluorescence microscope controlled by Slidebook Software. Fluorescence emission at 505 nm was monitored while alternating between 340 and 380 nm excitation wavelengths at a frequency of 0.67 Hz; intracellular Ca^{2+} measurements are shown as 340/380 nm emission ratios obtained from groups (35 to 45) of single cells. Measurements shown are representative a minimum of three independent experiments.

Materials

The inhibitor 3,4-dichloropropioanilide (DCPA) was from ChemServices (West Chester, PA). Working solutions were made in ethanol at 1000x final concentration, with equal ethanol added to controls. The inactive congener 3,4-difluoropropioanilide was synthesized by fluorination of propionanilide methyl ester; the product was de-esterified and purified by column chromatography, with identification of the purified product by spectroscopy.

Results

Ca^{2+} homeostasis during osteoclast differentiation

Store-dependent and store-independent changes in cytosolic Ca^{2+} concentration were examined in human monocytes isolated from buffy coat as they differentiated into

osteoclasts in vitro (Fig 1A G). Cultures maintained in m-CSF were treated with RANKL to induce and support osteoclast differentiation for 1, 3, 7 or 11 days. At each of these time points, cultures were loaded with Fura 2 to measure basal cytosolic Ca^{2+} concentration (Fig 1A-G) and samples were collected for Western analysis (Fig 1H). Intriguingly, irrespective of the presence of extracellular Ca^{2+}, spontaneous Ca^{2+} fluxes were observed in a significant percentage of these cells (Fig 1A-E). Further, the percentage of cells exhibiting these spontaneous Ca^{2+} fluxes increased the longer cells were maintained in RANKL, reaching as high as 75% at day 11 (Fig 1F). To assess the capacity of these cells for store-operated Ca^{2+} entry, they were then treated with the Sarco/Endoplasmic Reticulum (SERCA) inhibitor thapsigargin in the absence of extracellular Ca^{2+} to deplete ER Ca^{2+} content. The subsequent addition of 1 mM Ca^{2+} revealed significant decreases in the amount of Ca^{2+} entry between 1 and 11 days after the addition of RANKL (Fig 1A-E,G). Interestingly, this decrease in the capacity for store-operated Ca^{2+} entry during osteoclast differentiation coincided with decreases in the expression of STIM1, STIM2 and Orai1 (Fig 1H). Hence, not only does RANKL induce Ca^{2+} oscillations (as previously shown; Kim et al, 2010), the current investigations reveal dramatic changes in both the expression and function of proteins involved in store-operated Ca^{2+} entry during RANKL-induced osteoclast differentiation.

Reduced expression of Orai1 reduces multinucleation of human osteoclasts in vitro

To assess the contributions of CRAC channels towards osteoclast differentiation, human monocytes were treated with Cy5-labeled Orai1 siRNA and differentiated in vitro into osteoclasts. Transfection efficiency with an siRNA cocktail was ~75% (Figure 2A), with the ~80% decrease in Orai1 protein by Western analysis (Figure 2B) suggesting that very little Orai1 was present in cells that were transfected. Orai1 mRNA was also measured in cells at the time of plating and after RANKL addition for 3, 7 and 11 days (Figure 2C). Orai1 mRNA relative to GAPDH was reduced 60% at day 3 but message levels increased over time, in keeping with loss of siRNA. Irrespective, transfection with Orai1 siRNA resulted in a 58% decrease in SOCe relative to control 11 days after RANKL addition. Interestingly, addition of RANKL had no effect on Orai1 at the RNA level (Figure 2D), distinct from what was observed for Orai1 protein expression (Figure 1H). Nevertheless, knockdown of Orai1 markedly reduced the number of multinucleated cells after 7 days (Figure 2E, histogram and arrows in middle photomicrograph); multinucleated syncytia are required for efficient bone degradation and reduced multinucleated cells are a characteristic of osteopetrosis (Blair et al, 2009). However, other properties of osteoclasts include induction of TRAP and TRAP activity was similar in control and Orai knockdown cultures (Figure 2E, arrowheads in photomicrograph), suggesting that the reduction in multinucleation is distal to induction of key osteoclast proteins.

Pharmacological inhibition of store-operated calcium entry (SOCe) reduces multinucleation of human osteoclasts

Previously we showed that the haloanilide DCPA blocks store-operated Ca^{2+} channel function in Jurkat cells with no effect on ER Ca^{2+} content (Lewis et al, 2008). DCPA also reduced SOCe in osteoclasts by 27.5% (n = 3; data not shown). Whether effects of DCPA result from direct modulation of store-operated Ca^{2+} channels was not known. To address

this, we examined HEK293 cells stably expressing Orai1 and transiently transfected with YFP-STIM1 and measured the effect of DCPA on CRAC current or I_{CRAC}. CRAC channel activity was measured in the whole cell clamp position after passively depleting Ca^{2+} stores via the presence of 10 mM EGTA in the patch pipette. In both control and DCPA-treated cells, CRAC current began to develop within 30 s of break-in (Figure 3A). However, CRAC currents began to close prior to reaching the peak in DCPA-treated cells, returning to baseline less than 4 minutes after break-in. Analysis of the current-voltage relationship between control and DCPA-treated cells did not show significant differences (Figure 3B). These observations demonstrate that DCPA is a bona-fide CRAC channel inhibitor, although its mechanism of action was not yet defined.

Figure 3 (C-G) show the effect of DCPA on human osteoclast differentiation 8 days after addition of RANKL. Osteoclast differentiation is demonstrated by multinucleated (>2 nuclei/cell) cells and TRAP activity (Figure 3D). DCPA was added at 1.0, 10 and 100 μM to identical cultures at the time of RANKL addition; 1.0 μM DCPA had minimal effect on the number of multinucleated $TRAP^{+}$ cells (Figure 3E), but there was a marked progressive reduction in the number of multi-nucleated cells at 10 μM and 100 μM DCPA (Figure 3F, G). Despite qualitative differences in cell clumping and other secondary features of the cultures, no differences in the TRAP activity were observed even at the highest concentration of inhibitor, in keeping with results of Orai knockdown (Figure 2). The inactive DCPA congener 3,4-difluororopropioanilide (DFPA) (Lewis and Barnett, unpublished data) had no significant effect on multinucleation at either 10 μM (Figure 3I) or 100 μM (Figure 3H, I), indicating that DCPA-mediated inhibition of osteoclast formation results from CRAC inhibition.

DCPA reduces puncta formation by CRAC channel components in wild-type HEK293 cells or HEK293 cells overexpressing STIM1 and Orai1

Based on the investigation above, we were confident that DCPA inhibits CRAC-mediated Ca^{2+} influx. However, that no significant differences in the current/voltage relationship of I_{CRAC} were observed (Figure 3B) argues against a direct effect of DCPA on the Orai1 selectivity filter. Therefore, we performed a series of experiments to test the possibility that DCPA inhibits STIM1-Orai1 interaction. When ER Ca^{2+} stores are depleted, Ca^{2+} is released from the STIM1 EF-hand leading to its aggregation near the plasma membrane in structures often referred to as puncta. Therefore, we examined HEK293 cells transiently transfected with YFP-STIM1 to determine the effect of DCPA on STIM1 puncta formation using fluorescence microscopy. Prior to treatment, all cells displayed a diffuse distribution of YFP- STIM1 (Figure 4A, upper left panel). However, depletion of ER Ca^{2+} stores with 2 μM thapsigargin led consistently to extensive puncta formation in control cells within 7.5 minutes (Figure 4A, upper right panel). In contrast, DCPA treatment dramatically inhibited puncta formation after depleting Ca^{2+} stores over a 16 minute period (Figure 4A; bottom panels). Hence, a relatively small number of puncta appeared in specific locations (marked with an arrow), but the overall distribution of YFP-STIM1 in DCPA-pretreated cells was considerably more diffuse than control cells (Figure 4A, right panel). Considered in combination with our CRAC measurements (Figure 3A,B), these findings are consistent with an effect of DCPA on STIM1 aggregation and/or interaction with Orai1.

Recently, we demonstrated that, in cells overexpressing both Orai1 and the cytosolic fragment of STIM1 ($STIM1_{CT}$), a second CRAC channel modulator, 2-aminoethoxydiphenylborate (2-APB), causes $STIM1_{CT}$ to translocate to the plasma membrane and interact with Orai1 (Wang et al, 2009). To determine if DCPA modulates interactions between STIM1 and Orai1, a similar experiment was done in the presence or absence of DCPA. As depicted in Figure 4B (bottom left), YFP-$STIM1_{CT}$ was evenly distributed throughout the cytoplasm prior to the addition of 2-APB (50 μM). As early as 5 seconds after the addition of 2-APB, significant translocation of $STIM1_{CT}$ towards the PM could be seen (Figure 4B; top right panel). This effect is summarized in the top left panel of Figure 4B; $STIM1_{CT}$ remains localized to the plasma membrane for at least several minutes after addition of 2-APB. However, when this experiment was repeated in the presence of DCPA (100 μM), the ability of 2-APB to induce $STIM1_{CT}$ translocation to the plasma membrane was dramatically attenuated (Figure 4C). As such, our data indicates that DCPA inhibits STIM1/Orai1 interaction, likely by inhibiting STIM1 aggregate formation.

Discussion

In this study, we demonstrate marked changes in Ca^{2+} homeostasis during RANKL-mediated osteoclast differentiation. Interestingly, coincident with an increase in spontaneous Ca^{2+} oscillations (consistent with prior studies; Kim et al, 2010), we observed decreased functional activity and expression of the CRAC channel components, Orai1, STIM1 and STIM2. However, this did not reflect a reduced role for Orai1 in differentiating osteoclasts; either reducing Orai1 expression with small interfering RNA or interfering with its function using DCPA markedly inhibited osteoclast differentiation. Indeed, osteoclast differentiation, particularly multinucleation, occurred at very low rates when Orai expression and/or activity were suppressed.

The addition of RANKL caused complex changes in Ca^{2+} homeostasis; apparently spontaneous Ca^{2+} oscillations were observed throughout the differentiation period, events which coincided with significant changes in the expression and function of the SOCe components STIM1 and Orai1 (Figure 1). Although our observation of a role for SOCe in multinucleation is new. RANKL-induced Ca^{2+} oscillations in differentiating osteoclasts have been reported previously (Kim et al, 2010). In that study, Ca^{2+} oscillations were attributed to $InsP_3R$ activity downstream of RANK-dependent ROS production. Our findings are highly consistent with this interpretation, since Ca^{2+} fluxes could be observed in cells for as long as 30 min after removal of extracellular Ca^{2+} (data not shown). These observations are also highly consistent with previous work by our group, showing that osteoclast differentiation is highly Ca^{2+}-dependent, requiring expression of the $InsP_3R$ (Blair et al, 2007) to mediate the activation of NFATc1, the critical player in osteoclastogenesis (Day et al, 2005). What is both new and novel about the current study is the finding that SOCe is specifically required for terminal differentiation, yet dispensable for earlier events in osteoclast differentiation.

In studies where NFATc1 expression was silenced or over-expressed (Ikeda et al, 2006; Chang et al, 2008; Takayanagi et al, 2002), changes in osteoclast generation correlated directly with similar changes in the number of $TRAP^+$ cells. In the studies reported herein,

blockage of Ca^{2+} influx inhibited multinucleation but did not inhibit TRAP-activity. A potential explanation for this difference would be that the spontaneous and extracellular Ca^{2+}-independent Ca^{2+} fluxes that were observed throughout the osteoclast differentiation period are sufficient to activate NFATc1 and induce TRAP expression, but insufficient to induce cell fusion. It is interesting to note that the plasma membrane Ca^{2+} channel TRPV4 has also been shown to be important for terminal differentiation in osteoclasts (Masuyama et al, 2008). However, *trpv4*$^{-/-}$ mice differ significantly in phenotype from *Orai1*$^{-/-}$ in that *trpv4*$^{-/-}$ show increased bone mass attributed to reduced bone resorption, whereas *Orai1*$^{-/-}$ show poor bone development (Robinson et al., unpublished data). Irrespective, considered collectively, it seems clear that whereas early events in osteoclastogenesis depend on $InsP_3R$ and ROS (Blair et al, 2007, Day et al, 2005, Kim et al, 2010), osteoclast fusion is highly dependent on extracellular Ca^{2+}.

In prior studies, we established that DCPA can inhibit store-operated Ca^{2+} entry, although the mechanisms whereby this was achieved were entirely unclear (Xie et al, 1997; Ustyugova et al, 2007; Lewis et al, 2008). In addition to demonstrating its potential as an inhibitor of osteoclastogenesis, we have now shown that the channels inhibited by DCPA are specifically CRAC channels. We further show that this inhibition results from interference of STIM-Orai interaction. Precisely how this interference is achieved is unclear, but further characterization of this phenomenon may provide valuable new insight into the characteristics of STIM-mediated activation of Orai channels.

In conclusion, we demonstrate that the CRAC channel is a Ca^{2+} channel required for normal osteoclast differentiation in vitro. Further, based on our demonstrated effect of DCPA on SOCe via inhibition of STIM1 puncta, siRNA knockdown of Orai1 and the lack of an effect of these treatments on TRAP staining in monocytes after RANKL and m-CSF stimulation, we conclude that induction of TRAP activity is not dependent on extracellular Ca^{2+}. In contrast, multinucleation, another key characteristic of osteoclast differentiation, is dependent on functional CRAC channels, as depicted in Figure 5. As such, the current investigations have provided valuable new insight into both the roles of Ca^{2+} in osteoclast differentiation and the abilities of Ca^{2+} channel inhibitors to impact on this process. Given the critical role of osteoclasts in osteoporosis, osteopetrosis and bone degradation associated with arthritis, these findings may have significant therapeutic implications.

Acknowledgments

Funded in part by the National Institutes of Health (USA) awards ES011311, AG12951 and AR053566, and by the Department of Veteran's Affairs (USA). T.L.L. is an Environmental Protection Agency Greater Research Opportunity Fellow (MA-91684801-0). We thank Dr. Peter Gannett, Department of Medicinal Chemistry, West Virginia University School of Pharmacy, for synthesizing and purifying 3,4 difluoropropioanilide.

Literature Cited

Blair HC, Yaroslavskiy BB, Robinson LJ, Mapara MY, Pangrazio A, Guo L, Chen K, Vezzoni P, Tolar J, Orchard PJ. Osteopetrosis with micro-lacunar resorption because of defective integrin organization. Lab Invest. 2009; 89:1007–1017. [PubMed: 19546854]

Blair HC, Schlesinger PH, Huang CL, Zaidi M. Calcium signalling and calcium transport in bone disease. Sub-cellular biochemistry. 2007; 45:539–562. [PubMed: 18193652]

Chang EJ, Ha J, Huang H, Kim HJ, Woo JH, Lee Y, Lee ZH, Kim JH, Kim HH. The JNK-dependent CaMK pathway restrains the reversion of committed cells during osteoclast differentiation. Journal of Cell Science. 2008; 121:2555–2564. [PubMed: 18650497]

Day CJ, Kim MS, Lopez CM, Nicholson GC, Morrison NA. NFAT expression in human osteoclasts. J Cell Biochem. 2005; 95:17–23. [PubMed: 15759284]

Deng X, Wang Y, Zhou Y, Soboloff J, Gill DL. STIM and Orai: Dynamic Intermembrane Coupling to Control Cellular Calcium Signals. J Bio Chem. 2009; 284:22501–22505. [PubMed: 19473984]

Feske S. ORAI1 and STIM1 deficiency in human and mice: roles of store-operated Ca2+ entry in the immune system and beyond. Immunol Rev. 2009; 231:189–209. [PubMed: 19754898]

Feske S, Gwack Y, Prakriya M, Srikanth S, Puppel SH, Tanasa B, Hogan PG, Lewis RS, Daly M, Rao A. A mutation in Orai1 causes immune deficiency by abrogating CRAC channel function. Nature. 2006; 441:179–185. [PubMed: 16582901]

Ikeda F, Nishimura R, Matsubara T, Hata K, Reddy SV, Yoneda T. Activation of NFAT signal in vivo leads to osteopenia associated with increased osteoclastogenesis and bone-resorbing activity. J Immunol. 2006; 177:2384–2390. [PubMed: 16888000]

Kim K, Kim JH, Lee J, Jin HM, Lee SH, Fisher DE, Kook H, Kim KK, Choi Y, Kim N. Nuclear factor of activated T cells c1 induces osteoclast-associated receptor gene expression during tumor necrosis factor-related activation-induced cytokine-mediated osteoclastogenesis. J Biol Chem. 2005; 280:35209–35216. [PubMed: 16109714]

Kim K, Lee SH, Ha KJ, Choi Y, Kim N. NFATc1 induces osteoclast fusion via up-regulation of Atp6v0d2 and the dendritic cell-specific transmembrane protein (DC-STAMP). Mol Endocrinol. 2008; 22:176–185. [PubMed: 17885208]

Kim MH, Shim KS, Kim SH. Inhibitory effect of cantharidin on osteoclast differentiation and bone resorption. Arch Pharm Res. 2010; 33:457–462. [PubMed: 20361312]

Koga T, Inui M, Inoue K, Kim S, Suematsu A, Kobayashi E, Iwata T, Ohnishi H, Matozaki T, Kodama T, Taniguchi T, Takayanagi H, Takai T. Costimulatory signals mediated by the ITAM motif cooperate with RANKL for bone homeostasis. Nature. 2004; 428:758–763. [PubMed: 15085135]

Lewis TL, Brundage KM, Brundage RA, Barnett JB. 3,4-Dichloropropionanilide (DCPA) Inhibits T Cell Activation by Altering the Intracellular Calcium Concentration Following Store Depletion. Toxicological Sciences. 2008; 103:97–107. [PubMed: 18281253]

Li X, Hunter D, Morris J, Haskill JS, Earp HS. A calcium-dependent tyrosine kinase splice variant in human monocytes. Activation by a two-stage process involving adherence and a subsequent intracellular signal. J Biol Chem. 1998; 273:9361–9364. [PubMed: 9545257]

Liou J, Kim ML, Do HW, Jones JT, Myers JW, Ferrell JE Jr. Meyer T. STIM Is a Ca(2+) Sensor Essential for Ca(2+)-Store-Depletion-Triggered Ca(2+) Influx. Curr Biol. 2005; 15:1235–1241. [PubMed: 16005298]

Ma H-T, Patterson RL, van Rossum DB, Birnbaumer L, Mikoshiba K, Gill DL. Requirement of the Inositol Trisphosphate Receptor for Activation of Store-Operated Ca^{2+} Channels. Science. 2000; 287:1647–1651. [PubMed: 10698739]

Masuyama R, Vriens J, Voets T, Karashima Y, Owsianik G, Vennekens R, Lieben L, Torrekens S, Moermans K, Vanden Bosch A, Bouillon R, Nilius B, Carmeliet G. TRPV4-mediated calcium influx regulates terminal differentiation of osteoclasts. Cell Metab. 2008; 8:257–265. [PubMed: 18762026]

Muik M, Fahrner M, Derler I, Schindl R, Bergsmann J, Frischauf I, Groschner K, Romanin C. A Cytosolic Homomerization and a Modulatory Domain within STIM1 C Terminus Determine Coupling to ORAI1 Channels. J Biol Chem. 2009; 284:8421–8426. [PubMed: 19189966]

Park CY, Hoover PJ, Mullins FM, Bachhawat P, Covington ED, Raunser S, Walz T, Garcia KC, Dolmetsch RE, Lewis RS. STIM1 Clusters and Activates CRAC Channels via Direct Binding of a Cytosolic Domain to Orai1. Cell. 2009; 136:876–890. [PubMed: 19249086]

Robinson LJ, Yaroslavskiy BB, Griswold RD, Zadorozny EV, Guo L, Tourkova IL, Blair HC. Estorgen inhibites RANKL-stimulated osteoclastic differentiation of human monocytes through estrogen and RANKL-regulated interaction of extrogen receptor-alpha with BCAR1 and Traf6. Exp Cell Res. 2009; 315:1287–1301. [PubMed: 19331827]

Roos J, DiGregorio PJ, Yeromin AV, Ohlsen K, Lioudyno M, Zhang S, Safrina O, Kozak JA, Wagner SL, Cahalan MD, Velicelebi G, Stauderman KA. STIM1, an essential and conserved component of store-operated Ca2+ channel function. J Cell Biol. 2005; 169:435–445. [PubMed: 15866891]

Stathopulos PB, Li GY, Plevin MJ, Ames JB, Ikura M. Stored Ca2+ depletion-induced oligomerization of STIM1 via the EF-SAM region: An initiation mechanism for capacitive Ca2+ entry. J Biol Chem. 2006; 281:35855–35862. [PubMed: 17020874]

Stathopulos PB, Zheng L, Li GY, Plevin MJ, Ikura M. Structural and mechanistic insights into STIM1-mediated initiation of store-operated calcium entry. Cell. 2008; 135:110–122. [PubMed: 18854159]

Takayanagi H, Kim S, Koga T, Nishina H, Isshiki M, Yoshida H, Saiura A, Isobe M, Yokochi T, Inoue J, Wagner EF, Mak TW, Kodama T, Taniguchi T. Induction and activation of the transcription factor NFATc1 (NFAT2) integrate RANKL signaling in terminal differentiation of osteoclasts. Dev Cell. 2002; 3:889–901. [PubMed: 12479813]

Ustyugova IV, Frost LL, VanDyke K, Brundage KM, Schafer R, Barnett JB. 3,4-Dichloropropionaniline Suppresses Normal Macrophage Function. Toxicol Sc. 2007; 97:364–374. [PubMed: 17355946]

Vig M, Beck A, Billingsley JM, Lis A, Parvez S, Peinelt C, Koomoa DL, Soboloff J, Gill DL, Fleig A, Kinet JP, Penner R. CRACM1 Multimers Form the Ion-Selective Pore of the CRAC Channel. Curr Biol. 2006; 16:1–7. [PubMed: 16401419]

Wang Y, Deng X, Zhou Y, Hendron E, Mancarella S, Ritchie MF, Tang XD, Baba Y, Kurosaki T, Mori Y, Soboloff J, Gill DL. STIM protein coupling in the activation of Orai channels. Proc Natl Acad Sci U S A. 2009; 106:7391–7396. [PubMed: 19376967]

Watson JM, Harding TW, Golubovskaya V, Morris JS, Hunter D, Li X, Haskill JS, Earp HS. Inhibition of the calcium-dependent tyrosine kinase (CDATK) blocks monocyte spreading and motility. J Biol Chem. 2001; 276:3536–3542. [PubMed: 11062241]

Wu MM, Buchanan J, Luik RM, Lewis RS. Ca2+ store depletion causes STIM1 to accumulate in ER regions closely associated with the plasma membrane. J Cell Biol. 2006; 174:803–813. [PubMed: 16966422]

Xie YC, Schafer R, Barnett JB. The immunomodulatory effects of the herbicide propanil on murine macrophage interleukin-6 and tumor necrosis factor-alpha production. Toxicol Appl Pharmacol. 1997; 145:184–191. [PubMed: 9221836]

Yaroslavskiy BB, Zhang Y, Kalla SE, Garcia P, V, Sharrow AC, Li Y, Zaidi M, Wu C, Blair HC. NO-dependent osteoclast motility: reliance on cGMP-dependent protein kinase I and VASP. J Cell Sci. 2005; 118:5479–5487. [PubMed: 16291726]

Yi T, Lee HL, Cha JH, Ko SI, Kim HJ, Shin HI, Woo KM, Ryoo HM, Kim GS, Baek JH. Epidermal growth factor receptor regulates osteoclast differentiation and survival through cross-talking with RANK signaling. J Cell Physiol. 2008; 217:409–422. [PubMed: 18543257]

Yuan JP, Kim MS, Zeng W, Shin DM, Huang G, Worley PF, Muallem S. TRPC channels as STIM1-regulated SOCs. Channels (Austin). 2009; 3:221–225. [PubMed: 19574740]

Zhou Y, Mancarella S, Wang Y, Yue C, Ritchie M, Gill DL, Soboloff J. The Short N-terminal Domains of STIM1 and STIM2 Control the Activation Kinetics of Orai1 Channels. J Bio Chem. 2009; 284:19164–19168. [PubMed: 19487696]

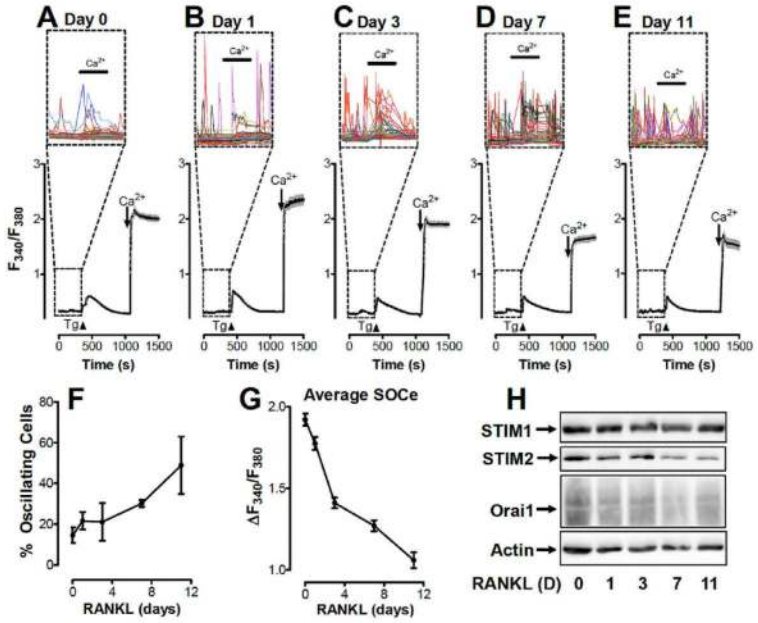

Figure 1. Modulation of store-operated calcium channels during osteoclast differentiation

A-E. Store operated calcium entry (SOCe) was measured in monocytes maintained in m-CSF (**A**; Day 0) supplemented with RANKL for 1 **(B)**, 3 **(C)**, 7 **(D)** or 11 **(E)** days. ER Ca^{2+} depletion via the addition of thapsigargin (Tg; 2 μM) in nominally Ca^{2+}-free medium. Extracellular Ca^{2+} concentration was increased from 0 to 1 mM either before or after store depletion where indicated to differentiate between store-independent (before Tg) and store-dependent (after Tg) Ca^{2+} entry. Each trace represents 30 to 40 cells, with the shaded areas indicating standard error (SEM). ***Insets:*** Each individual cell is depicted within the boxed regions to reveal Ca^{2+} fluxes during the period prior to the addition of Tg.

F. The percentage of cells exhibiting Ca^{2+} fluxes as depicted in panels **A-E** were determined in 4 experiments and averaged. Error bars show SEM.

G. The total amount of store operated Ca^{2+} entry at each time point is depicted. Averages are based on 125 to 175 cells collected during 4 experiments performed as depicted above **(A-E)**. Error bars show SEM.

H. Western blots for STIM1, STIM2, Orai1 and Actin in isolated monocytes maintained in m-CSF (day 0) and supplemented with RANKL for 1, 3, 7 or 11 days.

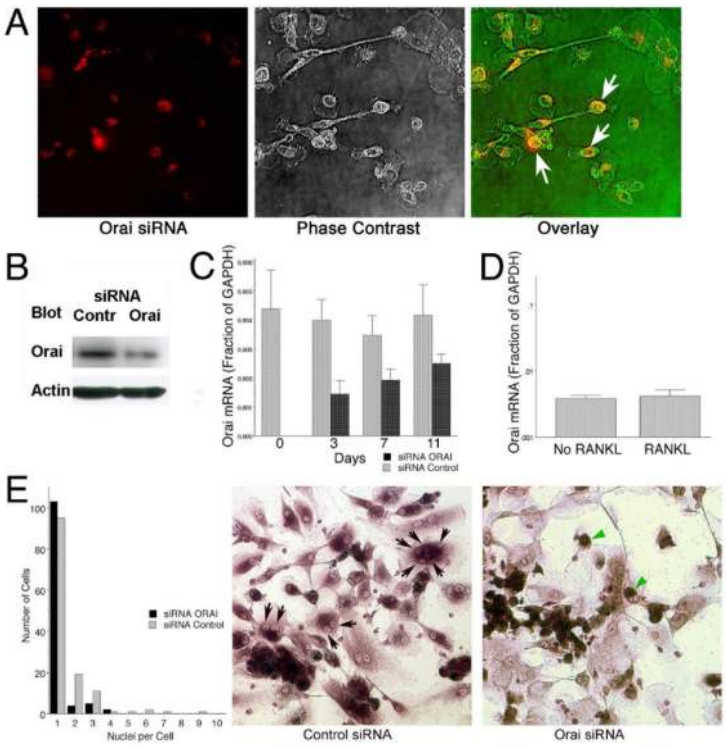

Figure 2. siRNA knockdown of Orai inhibits human osteoclast development in vitro

A. Transfection of a mixture of four siRNAs to reduce Orai1 expression was performed. Transfection with fluorescently tagged siRNA was used to allow efficiency to be monitored; this is shown one day after transfection (red signal, left) compared with phase to show the cells (middle frame) and the two overlain (phase in the red channel in this case, right). Approximately 75% of cells were transfected with detectable amounts of siRNA.

B. Three days after transfection of siRNAs Orai1 protein was determined by Western blot, relative to controls transfected with scrambled siRNA. The primary antibody was diluted 1:200 and the secondary anti-antibody was used at a 1:1000 dilution. The siRNA reduced Orai1 by ~80%.

C. Orai1 mRNA was quantified in transfected and control cells relative to GAPDH by quantitative real-time PCR as a function of time. After three days, mRNA is reduced ~60% but the siRNA was then progressively lost.

D. Treatment of cell cultures for seven days with RANKL relative to the same medium without RANKL did not affect Orai1 mRNA level relative to GAPDH, suggesting that expression is not down regulated by osteoclast differentiation.

E. Cells with Orai1 knocked down produce few multinucleated cells; the graph in the left frame shows summaries of cell number versus nuclei per cell from high power fields from four separate cultures of control or Orai1 knockdown cells, each field containing each ~30 cells. Cells were maintained in osteoclast differentiation medium, with RANKL and m-CSF, for seven days after transfection. Multinucleated cells are reduced ~70% by knockdown and very few cells with more than three nuclei were present (black bars) relative to controls (grey bars). Representative fields from control and Orai1 knockdown cells stained for TRAP activity are shown in the middle and right frames. Features include that there are

mononuclear cells with TRAP expression in the Orai1 knockdown (green arrows), but very few multinucleated cells are present relative to the control (black arrows, middle frame, indicate some nuclei in multinucleated cells).

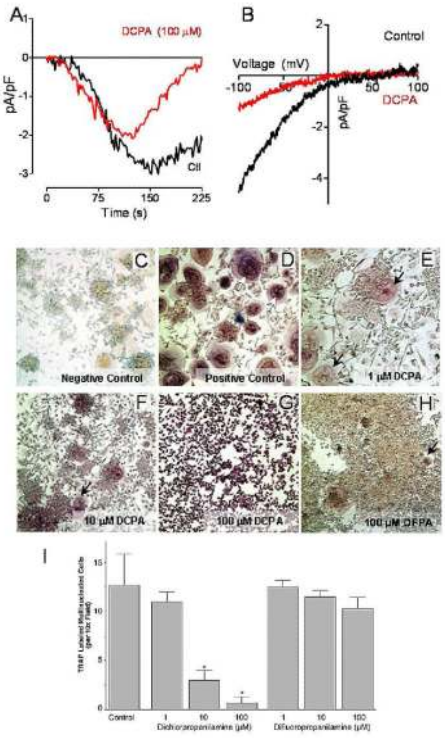

Figure 3. Pharmacological CRAC channel inhibition blocks osteoclast differentiation

(A) Time-course of whole-cell current measurement in 10 mM Ca^{2+} in HEK293 cells stably overexpressing Orai1 and transfected with STIM1 (-100 mV holding potential). Cells were pretreated for ~10 min with DCPA (100 μM) or DMSO (Control). Traces represent the average of 3 separate experiments.

(B) Current-voltage (I/V) relationships of CRAC currents extracted from representative cells shown in panel A at maximal current density revealing typical CRAC channel properties. Data represent leak-subtracted currents evoked by 50 ms voltage ramps from −100 to +100 mV, normalized to cell capacitance (pA/pF).

(C-G) Human monocytes were induced to differentiate by the addition of RANKL and m-CSF as described in the Materials and Methods. **(C**) A representative photomicrograph of cells after 8 days of culture without RANKL/m-CSF (negative control) and **(D**) with optimal concentrations of RANKL/m-CSF (positive control). Photomicrographs E through F shows the effect of blocking CRAC channel Ca^{2+} influx by the addition of graded concentrations of 3,4-dichloropropioanilide (DCPA). **(E**) DCPA, 1 μM had no effect on osteoclast differentiation, **(F**) 10 μM showed some inhibition of osteoclast differentiation and **(G**) 100 μM completely inhibited multinucleation of osteoclasts, while TRAP production was similar to control cells. **(H)** The inactive congener DFPA (100 μM) did not affect osteoclast differentiation, consistent with its inability to affect store operated calcium entry (Lewis and Barnett, unpublished data). **(I)** Numbers of TRAP positive, multinucleated cells (per 10× field) in monocyte cultures treated with RANKL, m-CSF and either DCPA or DFPA.

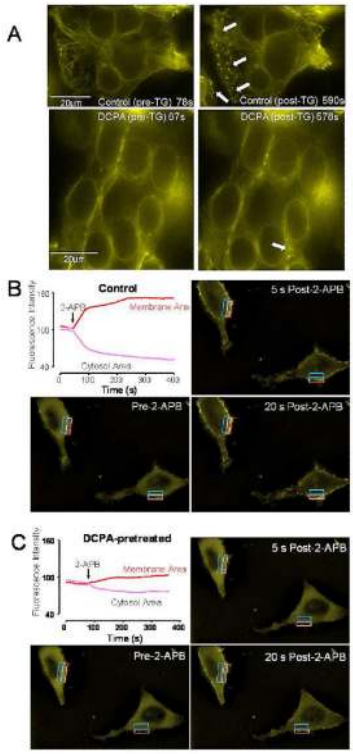

Figure 4. Effects of pharmacological inhibitors on STIM1 puncta formation and calcium currents in HEK293 cells

A. The store-operated calcium inhibitor DCPA inhibits puncta formation by the CRAC channel component, STIM1. The top two photomicrographs, show HEK293 cells, transfected with YFP-STIM1, that were stimulated with 2 μM thapsigargin (TG) at 78 seconds and images collected for 963 seconds and an average of 35 cells were observed. A representative image (60X) from a single focal plan for all images is shown. In the top right panel, the arrows point to areas of puncta formation within a single representative field. The bottom photomicrographs shows the effect of pretreating the cells with DCPA on STIM1 puncta formation. These cells were treated with 100 μM DCPA and were stimulated with 2 μM TG at 67 seconds and images were collected for 968 seconds. The bottom left photomicrograph was taken just before stimulating the cells with TG (67s). The bottom right photomicrograph taken at 578s, shows a diffuse pattern of fluorescence in the areas of the membrane where the development of puncta would be expected, as indicated by the arrows. **B-C.** Time-course of redistribution of STIM1-CT-YFP fluorescence induced by a second pharmacological inhibitor of SOCe, 2-APB (50 μM) in HEK293 cells stably expressing Orai1 and transfected with STIM1-CT-YFP. **(B**) Changes induced by 2-APB in STIM1-CT-YFP fluorescence at the membrane (red trace; outlined in white on the photomicrograph) or within the cytosol (blue trace; outlined in blue on the photomicrograph). The three photomicrographs were taken just prior to the addition of 2ABP and then 5 and 20s later. Beginning with the addition of 2-ABP, STIM1-CT-YFP fluorescence moved from an approximate equal distribution between cytosol and membrane to a predominantly membrane associated position. **(C**) Inhibition of 2-APB-induced association of the C-terminal YFP-tagged STIM fragment by DCPA. After an ~10 minute incubation in DCPA

(100 μM), 2-APB induced redistribution of STIM1-CT YFP fluorescence was determined. As shown by the graph (Figure 4C, top left) DCPA inhibited the redistribution on the fluorescence to the membrane area. Three photomicrographs were taken as the same time points described in B, i.e., just prior to the addition of 2ABP and then 5 and 20s later. The redistribution of STIM1-CT-YFP fluorescence, beginning with the addition of 2-ABP, showed substantially less redistribution between cytosol and membrane than the control group shown in (B).

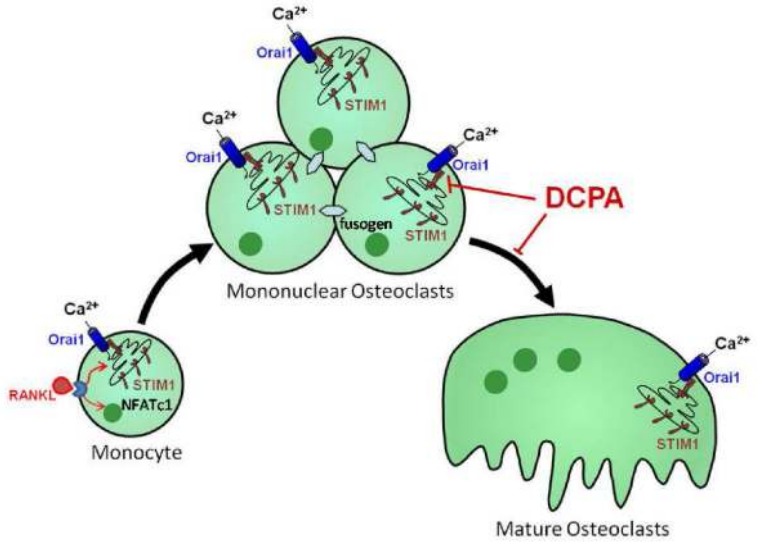

Figure 5. Model of the role of CRAC channels in osteoclast differentiation

Two store-operated Ca^{2+} entry (SOCe) events are required for m-CSF plus RANKL stimulation of osteoclast differentiation. The early SOCe through CRAC channels is postulated to activate NFATc1 through Ca^{2+}-dependent signaling pathways. The second (later) SOCe via CRAC channels (Orai1/STIM1) occurs at the time when mononuclear osteoclasts merge into multinucleated forms characteristic of fully differentiated osteoclasts. The role of SOCe at the later stage is postulated to be required to activate Ca^{2+}-dependent fusogens. These fusogens cause the formation of multinucleation required for osteoclast function. DCPA is a novel pharmacological inhibitor of STIM1 puncta formation as shown. The inhibition of STIM1 puncta formation prevents the formation of an active CRAC channel, thus, inhibiting terminal differentiation of the mononuclear osteoclasts into mature multinuclear osteoclasts.